IranJOC
Iranian Journal of Organic Chemistry

Synthesis, characterization and properties of hydrogel based on acrylic acid for removal of zinc ion from wastewater

Arman Samadzadeh Mamaghani, Mohammad Reza Manafi* and Mohammad Hojjati

Department of Applied Chemistry, Faculty of Science, South Tehran Branch, Islamic Azad University, Tehran, Iran

Abstract: This research investigated the PMA-AA (maleic acid/acrylic acid) hydrogel, which was synthesized by free radical polymerization of maleic acid / acrylic acid as monomers, using MBA as a Cross-linking agent and $(NH_4)_2S_2O_8$ as an initiator at 60 °C. FTIR and TGA spectroscopy were used to characterize the hydrogel. The FTIR results showed a large absorption band at 3000 cm^{-1} due to the stretching vibration of OH of AA and MA carboxylic functional groups. The absorption band of the C=O group at 1706 cm-1 in PMA-AA hydrogel disappeared with loaded Zn2+ ions. The C=O stretch frequency at 1631 cm-1 in PMA-AA hydrogel moved to 1629 cm-1; these variations in IR frequency indicate that hydrogel absorption is a chemical process. Hydrogel results showed no weight loss up to 155 °C free hydrogel but at 190 °C, suggesting the decomposition of the hydrogel backbone. This rapid weight loss for hydrogels loaded at 330 °C demonstrated an enhancement in the thermal stability of the hydrogel adsorb the heavy metals. It was determined that the concentration, temperatures, and time of the adsorption and adsorption capacity were studied in detail. The maximum sorption capacity was determined to be 239.89 mg/g. Langmuir isotherm provided the best explanation for the current outcome. The pseudo-second-order kinetic model well-represented sorption. Thermodynamic analysis shows that the adsorption of Zn^{2+} is exothermic. PMA-AA hydrogel loaded with Zn^{2+} ions desorbed was shown excellent regeneration performance and maintained 99.30% adsorption capacity after four adsorption–desorption cycles.

Keywords: Synthesis, Hydrogel, Adsorption, Free radical polymerization, Heavy metals.

Introduction

Synthesis of hydrogel compounds is a highly demanding field for chemists in organic chemistry (for selected examples of hydrogel synthesis); see [1]. A particularly efficient method in this field is free radical polymerization, a reaction between acrylic and maleic acid that has been described. This is a proper one-pot method for the synthesis of hydrogel from readily available starting materials (Scheme **1**).
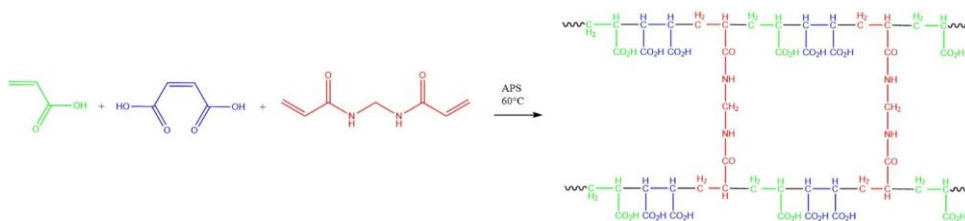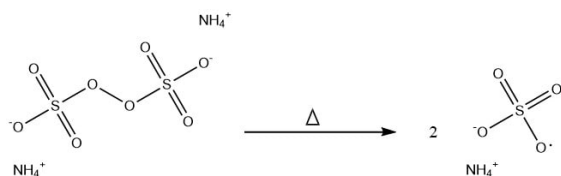

Scheme 1. Synthesis of Hydrogel based on acrylic acid

*Corresponding author. E-mail: mr_manafi@azad.ac.ir

Free-Radical Polymerization
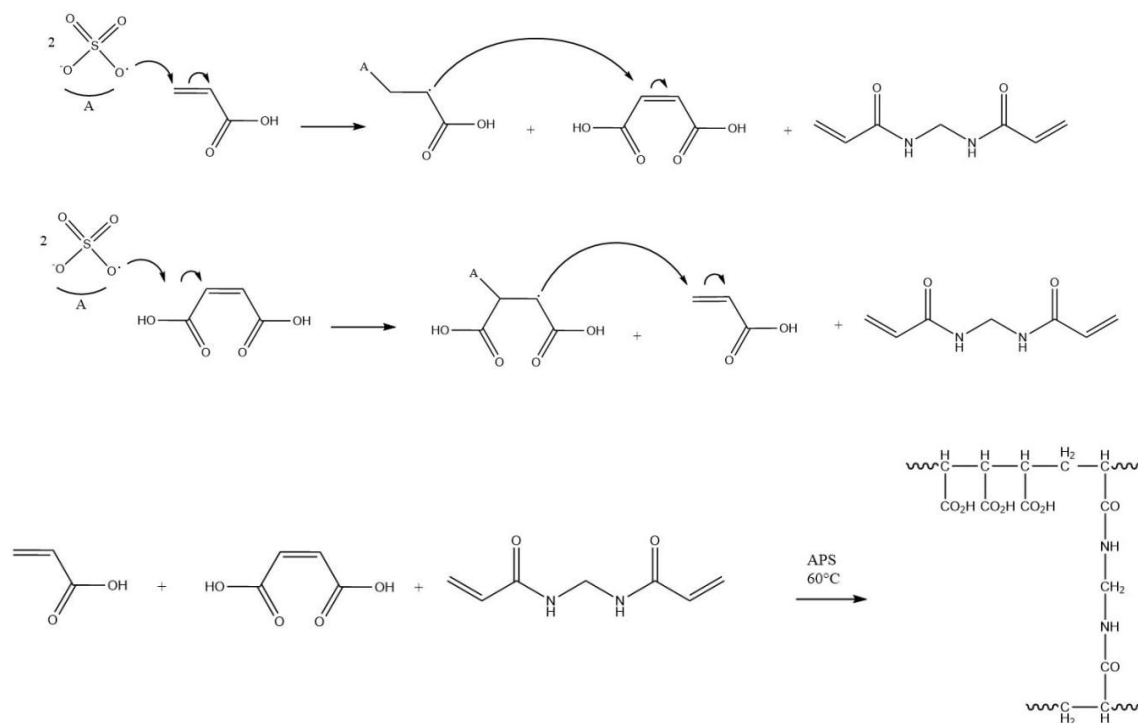
Initiators

The decomposition of the ammonium persulphate forms free radicals by heat energy. The way thermal decomposition takes place can be illustrated by Scheme **2**.

Scheme 2. Decomposition behavior of ammonium persulphate initiator at 60°C temperatures

Propagation

After 'initiation' comes 'propagation.' In the propagation step, the radical site at the first monomer unit attacks the double bond of a new monomer molecule. This results in the linking up of the second monomer unit to the first and the transfer of the radical site from the first monomer unit to the second by the unpaired electron transfer process. It should be noted that this chain still contains a radical site (indi-cated by a dot) at its end carbon atom and can, therefore, attack yet another monomer molecule (and thus take it on) with a simul-taneous transfer of the radical site to the new monomer unit added. This process involves a continuing attack on fresh monomer mole-cules, which, in turn, keep successively adding to the growing chain one after another. The propagation lasts until the chain growth is stopped by the free-radical site being 'killed' by some impurities, a sheer termination process, or until there is no further monomer left for the attack. As it is shown in Scheme **3**.

Scheme 3. Mechanism of preparation of hydrogel

Hydrogels can absorb vast quantities of water without dissolving in it. Hydrogels have excellent properties due to their softness and intelligence and can store water. Hydrogels cannot absorb much water because of their hydrophobic component, which is present in hydrogels produced by copolymerizing a hydrophilic monomer with a hydrophobic monomer that shows good mechanical strength. Toxic metals are present in groundwater. They are considered hazardous compounds because they are non-biodegradable, and their health hazards are proportional to their levels of exposure. Mercury (Hg), chromium (Cr), Copper (Cu),

zinc (Zn), cadmium (Cd), cobalt (Co), and nickel (Ni) are regularly detected in industrial effluent. Furthermore, these wastewaters combine with subsurface water sources [1, 2]. Regarding their toxicity, zinc has been selected as a typical element for this study. Zinc is essential for many enzyme systems that may produce severe diseases and pancreatic damage. Some methods are applied to eliminate heavy metal ions from wastewater, which include electrocoagulation [3, 4], Chemical precipitation [5], ion exchange [6], extraction [7], adsorption, etc., and are used to remove heavy metals from water. Activated carbon [8, 9], Carbon nanotubes [10], starch [11], clay [12], cellulose [13, 14], sawdust [15], chitosan [16, 17], etc., improved rheological properties of the nanocomposites of Poly (acrylamide-co-acrylic acid) and Carbon Nanotubes [18]. It has been observed that acrylic acid-based hydrogels combine with polyacrylamide PEG PVA etc. [19]. Synthesis of nanocomposites from polyacrylamide and graphene oxide: application as flocculants for water purification [20]. They are often used to eliminate toxic metals. However, these techniques also have disadvantages, including poor adsorption rates, reusability, less thermal stability, and insensitivity to acidity and temperature. Hydrogels can attract more in this setting due to their simple structure, low manufacturing costs, and reusability. Synthesis of poly (acrylamide-co-acrylic acid) as soil stabilizers and investigating its rheological properties copolymer based on acrylamide and acrylic acid was used in small-scale plots in experimental conditions for use in soil for its stabilization and preventing its loss [21]. Because of carboxylic acid side groups, polyacrylic acid hydrogel's swelling and absorption characteristics are high. Polyacrylic acid loses protons in the water, gets a negative charge, and functions as a polyelectrolyte. Due to the presence of ionic groups, polyelectrolyte hydrogels are sensitive to ionic strength, pH, temp, and other variables. Carboxylic groups generate complex structures within the polymer matrix that bind with metals and other environmental contaminants [22]. By changing the amount of the hydrophilic fraction of the hydrogel and the extent of cross-linking, particular qualities may be imparted to the hydrogel. Hydrogels based on poly acrylic acid absorbed heavy metals [23]. However, in the scientific literature, increasing the hydrophilicity of polyacrylic acid by copolymerization with additional hydrophilic monomers is rare since it decreases the material's mechanical strength. Therefore, we want to polymer the reaction of acrylic acid with maleic acid to create a polymer matrix with

excellent water-absorbance capabilities derived from hydrophilic monomers, which are employed to trap metals inside it. Furthermore, the hydrogels' mechanical strength was modified by adjusting the quantity of cross-linker. In this paper, the manufacture of poly (maleic acid-co-acrylic acid) hydrogel, also known as PMA-AA, was done, and its suitability for eliminating Zn^{2+} as a function of hydrogel compositions, also the temperature, treatment duration, and starting metal ion concentration. Water is abundant in nature, yet drinking water remains rare, despite being an urgent necessity. Therefore, the adsorption process may be promising for eliminating heavy metal ions from wastewater if a suitable adsorbent is used. Numerous hydrogels have been described with absorption, even in minutes [25, 26] or extremes in hours [27, 28]. However, this work describes a practical approach to absorbing up to 90% of heavy metals in 15 minutes. In addition, the unique quality of this produced gel exhibits complete desorption with no loss of activity; consequently, with a short time, adsorption and reusability are described as a practical and cost-effective wastewater treatment approach.

Results and discussion

Hydrogel composition and metal absorption

The hydrogel was synthesized by free radical polymerization of MBA as a Cross-linking agent and $(NH_4)_2S_2O_8$ as an initiator at 60°C. FTIR and TGA spectroscopy characterized the hydrogel, as shown in Figures 10 and 11. It was shown in Figure 1 Zn^{2+} ions in wastewater PMA-AA hydrogel can be used as a suitable adsorbent for effective elimination. This may be because of the inclusion of maleic acid, which increases the absorption capacity of PMA-AA hydrogel through two carboxylic groups. AA was neutralized to varying degrees (0–50%) with 5 M concentrated aqueous NaOH. The PMA-AA hydrogel with 50% neutralized acrylic acid had the most significant absorption, as shown in Figure 2. The COO^- and COOH of PMA-AA hydrogel interact electrostatically with metals. With neutralization, the COO^-/COOH ratio rises, which enhances the metal-hydrogel interaction. More significant electrostatic interaction exists between COO^- and metal ion than between COOH and metal ion.
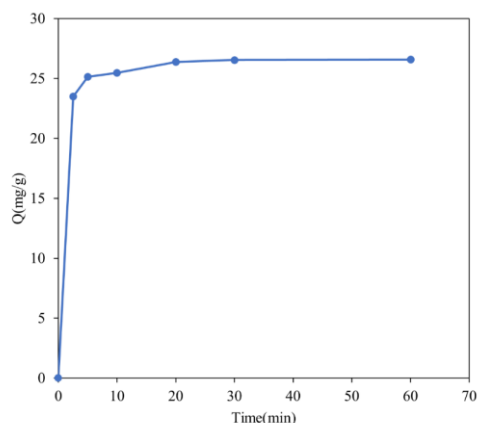
Figure 1. Adsorption capacity of PMA-AA hydrogels for Zn^{2+} (initial metal ion concentration = 10 mg/L)
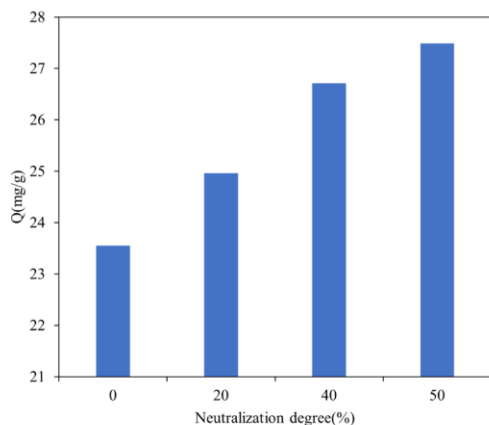

Figure 2. Effect of neutralization of AA on the adsorption capacity of PMA-AA hydrogel (initial metal ion concentration = 10 mg/L)

The Influence of Temperature on Metal Adsorption

To determine the influence of temperatures on sorption, PMA-AA hydrogel was maintained in metal solutions at several temperatures Figure **3**. The hydrogel's absorption capacity declined as the temperature rose from 18°C to 66°C. At higher temperatures, the activation rate and energy of metals increase, resulting in a greater tendency for metals to exit the hydrogel faster, reducing adsorption [30, 31].
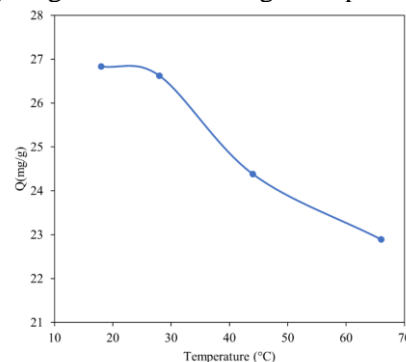
Figure 3. Effect of temperature on adsorption of Zn^{2+} by PMA-AA hydrogel (initial metal ion concentration = 10 mg/L).

Adsorption Isotherms

At room temperature, the free hydrogel was added to various concentrations of metal ions (10 to 1500 mg/L), and its absorption was evaluated. It is evident from Figure **4** that metal absorption in the initial concentration of metal rises dramatically and approaches equilibrium at around 10 ppm. It has also been shown in Table **1** that the sorption capacity of PMA-AA hydrogel with Zn^{2+}. Additionally, this information is also similar to the thermogram.
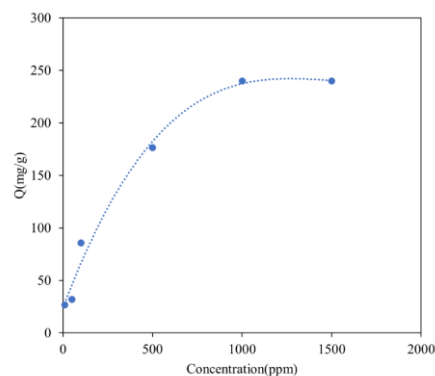
Figure 4. Equilibrium adsorption isotherm of Zn^{2+}

Table 1. Uptake of Zn^{2+} adsorption on PMA-AA

The initial concentration of metal ion solution (mg/L)	Amount of absorbed Zn^{2+} ions (mg/g)
10	26.61
50	31.9
100	85.88

500	176.49
1000	239.89
1500	239.89

Isotherm models may be used to study the adsorption mechanism by studying the interactions between hydrogel and metal ions. Langmuir, Freundlich, and Temkin are three extensively used isothermal adsorption models. The Langmuir isothermal model assumes that the adsorbent is monolayer adsorbed on the adsorbent surface and that the adsorption sites are equally distributed on the surface, so the adsorbed molecules do not interact with each other. R_L is a non-dimensional equilibrium sorption parameter in the Langmuir isotherm model [32]. The Freundlich isothermal model is an empirical equation implying that adsorption is multilayered on the adsorbent surface because the adsorption sites are not equally distributed on the adsorbent surface [33]. Temkin's isothermal model implies that the adsorbent and the adsorbent are mutually exclusive and that the heat of adsorption reduces linearly with increasing adsorbent surface coverage [34]. In this work, these models were fitted with the experimental data, and the adsorption mechanism of PMA-AA hydrogel on Zn^{2+} ions was studied. The equation below represents the Langmuir isothermal model:

$$q_e = \frac{q_{max} K_L C_e}{1 + K_L C_e} \qquad (1)$$

The following equation represents the separation factor R_L:

$$R_L = \frac{1}{1 + K_L C_0} \qquad (2)$$

The following equation represents the Freundlich isothermal model:

$$q_e = K_F C_e^{\frac{1}{n}} \qquad (3)$$

The following equation illustrates the Temkin isothermal model:

$$q_e = \frac{RT}{b_T} \ln(K_T C_e) \qquad (4)$$

Where C_0 and C_e are the initial and equilibrium concentration of the Zn^{2+} (mg/L), Q_e and Q_{max} are the adsorption equilibrium capacity and saturation of the sorbents (mg/g), K_L is the Langmuir adsorption equilibrium constant related to the binding energy (L/mg), and R_L is the separation factor, which can be used to determine whether it is suitable for absorption $(0 < R_L < 1)$, unfavorable absorption $(R_L > 1)$. K_F is the Freundlich adsorption equilibrium constant, and n is the adsorbed strength constant, which may be used to assess whether a substance is adsorbable. Favorable $(0 < 1/n < 0.5)$, unfavorable absorbing $(1/n > 2)$ K_T is the absorption equilibrium constant, b_T is the constant for the absorption heat, R is the gas constant (8.314 J/mol.K), and T is the absolute temperature (K). Table **2** shows the characteristics of the adsorption isotherm and correlation coefficient of Zn^{2+} ions. Figure **5** shows the results of the fitted curve for the isothermal model. Table 2 demonstrates that the Langmuir isotherm model best fits with the experimental data, as shown by a correlation coefficient greater than $R^2 > 0.973$. The adsorption of Zn^{2+} ions by PMA-AA hydrogel was determined to be monolayer adsorption, with a maximal theoretical adsorption capacity of 239.89 mg/g. Using the Langmuir isotherm model, the separation factor R_L (0.13, $0 < R_L < 1$) was obtained, indicating that the experimental condition was suitable for adsorption. In addition, the Freundlich isothermal model yielded a correlation parameter of 1/n (0.479, $0 < 1/n < 0.5$), indicating that absorption is also likely to occur.

Table 2. Constants of Langmuir and Freundlich and Temkin isotherm models for Zn^{2+}

Langmuir						Freundlich					Temkin					
R^2	Q_{max}	K_L	R_L	RMSE	$\Delta Q_e\%$	R^2	K_F	n	RMSE	$\Delta Q_e\%$	K_T(L/g)	bT	RT/b_T(J/mol)	R^2	RMSE	$\Delta Q_e\%$
0.973	277.778	0.004	0.13	12.628	37.009	0.933	8.013	2.084	19.021	30.415	0.10	51.591	47.242	0.9171	25.884	84.705
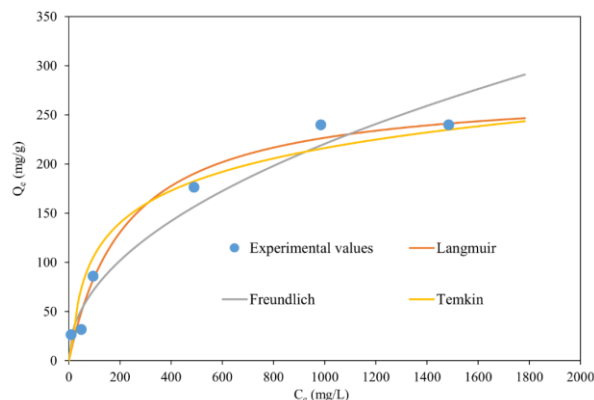
Figure 5. Langmuir, Freundlich and Temkin adsorption isotherms of Zn^{2+} by PMA-AA

The absorption capacity of PMA-AA hydrogel is shown in Table **3** based on the results of this investigation. The PMA-AA hydrogel has a more significant absorption potential for Zn^{2+} than other polyacrylic acid hydrogels.

Table 3. The metal ion sorption capacity of acrylic acid-based hydrogel prepared in the present work in comparison with that of some recently reported hydrogel

	Metal	**Q (mg/g)**	**Reference**
Poly (N-hydroxy methyl acrylamide-Co-Acrylic acid)	Zn	10.0	23
Collagen-g-poly (Acrylic acid)	Zn	51.65	36
Poly (maleic acid-co-acrylic acid)	Zn	239.89	Present work

Kinetic Research

Figure 1 is shown the absorption of metal ions vs time. It was observed that more than 90% of the metals were eliminated after 15 minutes, and the hydrogel was saturated with metal ions by 60 minutes [35, 37, 38]. The significant rise in the absorption rate indicates that the absorption occurs on the polymer's surface [27]. The quick absorption of metals by adsorption is of practical importance since it facilitates the safe, rapid, and inexpensive removal of undesirable metals. The absorption rate was determined using pseudo-first-order and pseudo-second-order kinetic models; the pseudo-first-order equation is [35].

$$\ln(Q_e - Q_t) = \ln Q_e - k_1 t \qquad (5)$$

Where Q_e and Q_t are the metal concentrations in the hydrogel at equilibrium (mg/g) and time t (min), respectively, and k_1 is the pseudo-first-order constant (min-1). The slope of plots of $\ln(Q_e - Q_t)$ with time revealed the rate constant (k_1). The value of Q_e was determined using the antilogarithm of the y-intercept. Figure **6**.
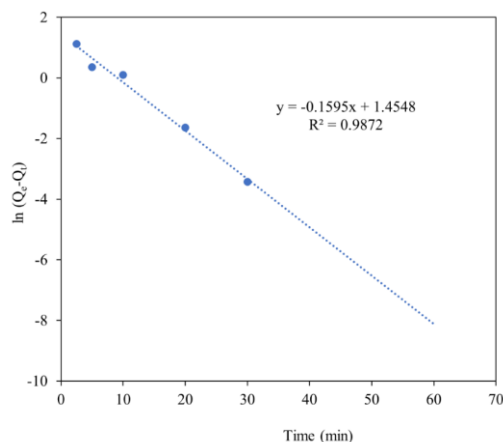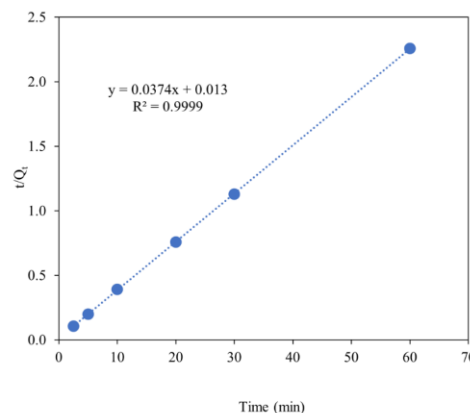

Figure 6. Pseudo-first-order kinetic plot for adsorption of Zn^{2+} ions on PMA-AA hydrogel.

The pseudo-second-order model is a kinetic model used to explain the adsorption process. The linear form of the pseudo-second-order equation is [35].

$$\frac{t}{Q_t} = \frac{1}{k_2 Q_e^2} + \frac{t}{Q_e} \qquad (6)$$

Table 4 contains the k_1, k_2, $h(=k_2 Q^2_e)$ values and the correlation analysis R^2 for pseudo-first and pseudo-second-order kinetic models from Figure **7**. In addition, the experimentally determined Q_e values are agreed with those predicted by the pseudo-second-order kinetic model. The correlation coefficient value of the pseudo-first-order model is less than that of the pseudo-second-order model, indicating that the pseudo-second-order kinetic model is better agreed than the pseudo-first-order kinetic model.

Figure 7. Pseudo-second-order kinetic plot for adsorption of Zn^{2+} ions on PMA-AA hydrogel.

Table 4. Kinetic parameters for the adsorption of Zn^{2+} on PMA-AA hydrogel

Pseudo-first-order						Pseudo-second-order					
Q_e	K_1	h_0	R^2	RMSE	$\Delta Q_e\%$	Q_e	K_2	h_0	R^2	RMSE	$\Delta Q_e\%$
4.28	0.1595	0.68	0.98	13.66	55.24	26.74	0.10760	76.92	0.99	0.11	0.43

Zn^{2+} adsorption and thermodynamic investigations influenced by adsorption temperature:

The effect of temperature on absorption was studied by varying the temperature from 18 to 66 °C. The Zn^{2+} adsorption capability of PMA-AA hydrogel at different temperatures is shown in Figure 3. The absorption capacity of PMA-AA decreased with increasing temperature, indicating that the absorption of Zn^{2+} ions by PMA-AA hydrogel might be exothermic.
To further study the influence of temperature on absorption, the thermodynamic characteristics of absorption were determined at four different temperatures (291, 301, 317, and 339 K). The Langmuir isotherm model fitted best with the experimental data. Therefore the Gibbs free energy change ΔG (kJ /mol), enthalpy change ΔH (kJ/mol), and entropy change ΔS (J/mol.K) may be calculated by using the equilibrium constant K_L [39]. The following is the formula:

$$\Delta G = -RT \ln K_L \qquad (7)$$

$$\ln K_L = -\frac{\Delta H}{RT} + \frac{\Delta S}{R} \qquad (8)$$

Where R represents the gas constant (8.314 J/mol.K), T represents the absolute temperature (K), and K_L represents the Langmuir adsorption equilibrium constant (L/mol). As illustrated in Figure 8, ΔH and ΔS may be derived from the slope and intercept plot of $\ln K_L$ vs $1/T$. The thermodynamic parameters and correlation coefficient of Zn^{2+} ions are reported in Table 5.

Negative ΔG of the adsorption reaction indicates the spontaneous nature of the adsorption of Zn^{2+} ions by hydrogels. As the temperature increased, ΔG progressively dropped, indicating that an increase in sorption temperature [40] favored the sorption of Zn^{2+} ions by hydrogels. The negative value of the ΔH of the adsorption reaction was -3.461 kJ/mol, indicating that the adsorption of Zn^{2+} ions by hydrogels is an exothermic process. The adsorption reaction exhibited a positive ΔS value of 55.382 J/mol.K, showing that the sorption of Zn^{2+} ions by hydrogels is a disorder-to-order process.

Table 5. Adsorption thermodynamic parameters for Zn^{2+} adsorption by PMA-AA hydrogel

ΔG (kJ/mol)				ΔH (kJ/mol)	ΔS (J/mol.K)	R^2
291 K	301 K	317 K	339 K			
-19.544	-20.192	-20.989	-22.238	-3.461	55.382	0.963
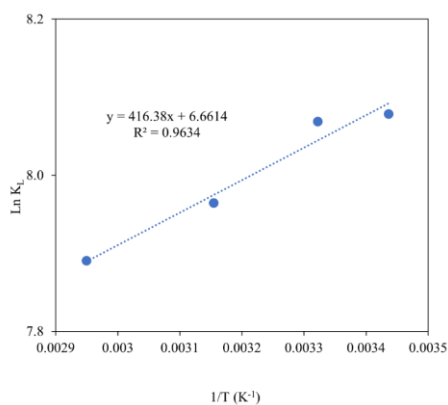
Figure 8. The plot of lnK_L versus 1/T for the adsorption of Zn^{2+} ions (initial concentrations: 10 mg/L, adsorption time: 1 h)

Desorption studies

Four cycles of adsorption-desorption tests were conducted to determine the hydrogel's reusability. Absorption investigations used metal solutions at a concentration of 10 ppm. for a desorbing 0.1N HCl was used. An acidic desorption agent was chosen because, at low pH, the binding site on the hydrogel will be protonated, causing H ions to compete with metal ions, hence decreasing the hydrogel's metal affinity. Figure **9** is shown the relation between the number of cycles and the hydrogel absorption capacity for Zn^{2+}. Even after four cycles, there is no noticeable decline in the absorption capacity of the regenerated hydrogel.
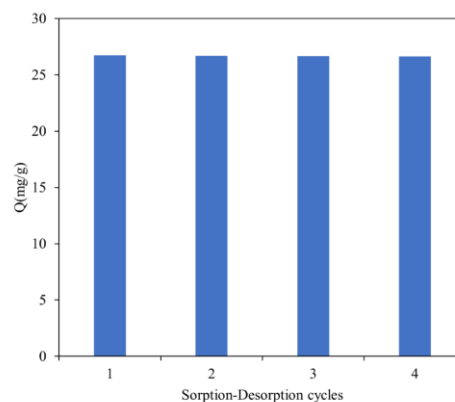
Figure 9. Relationship between Sorption-Desorption cycles and adsorption capacity of PMA-AA hydrogel for Zn^{2+} ions.

Hydrogel characterizations of PMA-AA, PMA-AA-Zn^{2+}

FTIR and TGA spectroscopy characterized the hydrogel with and without metal ions. As shown in Figures **10** and **11**.

We investigated the FTIR spectra of loaded hydrogel with and without metal ions to identify the interactions between the hydrogel and metal ions. The results are shown in Figure 10. In PMA-AA hydrogel, a large absorption band at 3000 cm^{-1} was found, correlating to the stretching vibration of OH groups, AA and MA carboxylic groups. After Zn loading, the significant absorption band of the C=O group at 1706 cm^{-1} in PMA-AA hydrogel disappeared. The C=O stretch frequency of the carboxyl group at 1631 cm^{-1} in PMA-AA hydrogel moved to 1629 cm^{-1}, respectively, in hydrogels containing Zn. C-O bending frequencies (1559 and 1359 cm^{-1}) were shifted to 1549 and 1407 cm^{-1} for Zn^{2+}. These variations in IR frequency indicate that hydrogel absorption is a chemical process. The hydrogel absorbs metals due to the COOH and COO$^-$ groups present in AA and MA.
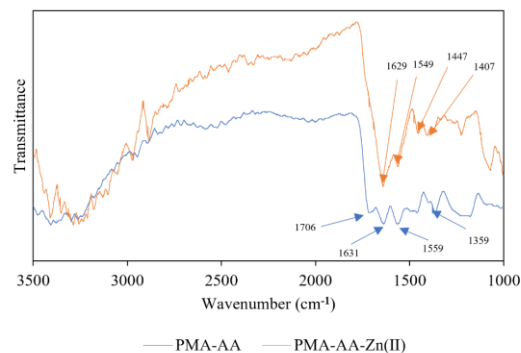
Figure 10. FTIR spectra of PMA-AA hydrogel before and after adsorption of Zn^{2+}

Figure **11** is the TGA graph of metal-free and metal-loaded PMA-AA hydrogel. It is the weight loss vs temperature. No weight loss was seen for free hydrogel up to 155 °C, but at 190 °C, a significant weight loss was found, suggesting the decomposition of the hydrogel backbone. This rapid weight loss for hydrogels loaded with Zn^{2+} at 330 °C enhanced the hydrogel's thermal stability following contact with heavy metals.
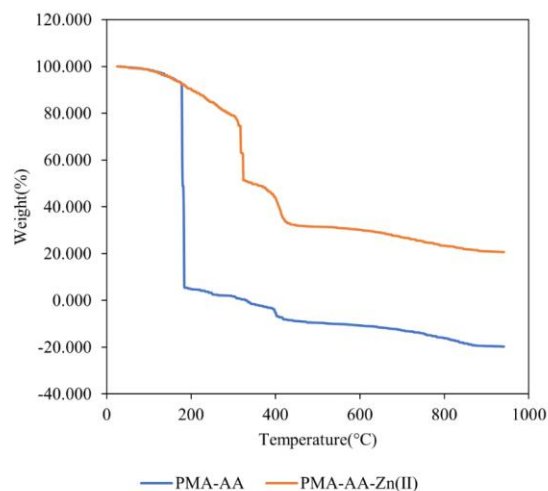
Figure 11. TGA measurements of PMA-AA hydrogel, PMA-AA-Zn^{2+}

Conclusions

This research investigated the PMA-AA hydrogel, which was synthesized by free radical polymerization, and it is an efficient metal ion adsorbent for eliminating Zn^{2+} from the aqueous phase. The effects of temperature, time, and metal ion concentration on absorption were studied. That indicated the equilibrium was attained within 60 minutes and the adsorption kinetics were determined to be pseudo-second-order kinetics. The results were evaluated using Langmuir,

Freundlich, and Temkin isotherms; however, the Langmuir model provided the best explanation for the current outcome with the regression value ($R^2 > 0.973$), and the maximum adsorption capacity was 239.89 mg/g. The adsorption capacity of Zn^{2+} with the TGA analysis was shown that the hydrogel's absorption capacity decreased as the temperature increased. Thermodynamic studies were shown that the adsorption of Zn^{2+} ions by PMA-AA hydrogels was an exothermic process; in addition, Zn^{2+} can be desorbed from the hydrogel by using 0.1 N HCl, and the adsorption capacity is unaffected by four cycles; as a result of PMA-AA and regeneration performance still maintained 99 30%.

Experimental

Materials and methods

The analytical quality maleic acid (MA), acrylic acid (AA), ammonium persulfate (APS) initiator, and N, N-methylene bis acrylamide (NMBA) cross-linker were acquired from Merk. They were used without any further purification. To the necessary degree, acrylic acid was neutralized with NaOH from Sigma-Aldrich, and all solutions were produced in deionized water. Additionally, zinc (II) chloride was obtained from Sigma-Aldrich.

Synthesis of PMA-AA Hydrogels

In 8 mL of water, 0.50 mol% NMBA and 1.60 mol% APS were dissolved. After adding 2 mL of neutralizing AA, the solution was sealed in the poly (vinyl chloride) end of a 20 cm long, 0.3 cm diameter straw. Two hours were spent heating the straw at 60 °C in an oven set [29]. Straws were removed from the oven and cooled to room temperature after the hydrogels were created. To eliminate unaltered species, the hydrogels were withdrawn from the straw, cut into cylindrical pieces, and immersed in deionized water for 5 to 6 hours. The water was changed every thirty minutes. The hydrogel was then dried at 40°C until its weight remained constant. The generated hydrogels were transparent, elastic, soft, and cylindrical and had a diameter of 0.1 cm and 2 cm in length. PMA-AA hydrogels are also produced using the same technique. Here, the ratio of MA to AA was 1:4. To test the impact of neutralization on the hydrogel's absorption capabilities, the AA neutralization level was changed from 0 to 50%.

Transform IR Fourier Measurements

The hydrogels were structurally characterized using a Fourier infrared spectrometer (Perkin Elmer, USA). Characterization was done before and after the

absorption of metal ions on the hydrogel, and also hydrogel spectra were taken to identify the interaction between the hydrogel and metal ions.

Thermal Gravimetric analysis

A thermogravimetric analyzer TGA2 (Mettler Toledo, Switzerland) is used to examine the hydrogel's heat stability with and without absorbed Zn^{2+}. A sample of 0.007 g was put in a platinum cup at temperatures ranging from 25 to 1,000 °C at a rate of 10°C/min in a nitrogen environment at a 100 mL/min flow rate.

Elimination of Zn^{2+}

Around 0.0125 g of hydrogel with a length of 0.1 cm immersed in 200 mL of known concentration of zinc solutions. At specified intervals, a predetermined volume of the solution was removed to analyze the metal concentration until equilibrium was attained. A spectrometer for atomic absorption (AAS) was used to assess metal concentrations. Test adsorption of the Zn^{2+} ions concentration using the graphite furnace atomic spectrometer (Agilent, USA). In all studies, the starting concentration of the metal solution was 10 mg/L, and all experiments were conducted at 25°C. The amount of adsorbed metal per unit weight of hydrogel at time t, Q (t) (mg/g), was obtained from the equation as [41].

$$Q(t) = \frac{\sum(C_0 - C_t)V_c}{m} \qquad (9)$$

C_0 and Ct are the initial metal concentration and concentration at time t in mg/L, Vt is the volume of solution per litre at time t, and m is the hydrogel weight in grams.

Desorption and Regeneration Studies

Hydrogel will be most beneficial if it can be desorbed and regenerated after usage. To study desorption, metal-loaded hydrogels were immersed in 20 mL of 0.1 N HCl at room temperature (25°C) for one hour. The ratio of desorption was then calculated as [42].

$$\text{Desorption ratio} = \frac{\text{(amount of metal ions desorbed into the elution medium)}}{\text{(amount of metal ions adsorbed on to the hydrogel)}} \qquad (10)$$

The hydrogel is then rinsed twice with water and introduced to recycled metal solutions. The sorbent-desorption procedure was carried out four times.

Acknowledgements

References

[1] Belkadi, S.; Bendaikha, H.; Lebsir, F.; Ould-Kada, S. *Orient. J. Chem.*, **2018**, *34*, 948.

[2] Kabir, S.; Sikdar, P. P.; Haque, B.; Bhuiyan, M.; Ali, A.; Islam, M. *Prog. Biomater.*, **2018**, *7*, 153-174.

[3] Ajiboye, T. O.; Oyewo, O. A.; Onwudiwe, D. C. *Chemosphere*, **2021**, *262*, 128379.

[4] Li, J.; Wang, X.; Zhao, G.; Chen, C.; Chai, Z.; Alsaedi, A.; Hayat, T.; Wang, X. *Chem. Soc. Rev.*, **2018**, *47*, 2322-2356.

[5] Shrestha, R.; Ban, S.; Devkota, S.; Sharma, S.; Joshi, R.; Tiwari, A. P.; Kim, H. Y.; Joshi, M. K. *Chem. Eng.*, **2021**, *9*, 105688.

[6] Bolisetty, S.; Peydayesh, M.; Mezzenga, R. *Chem. Soc. Rev.*, **2019**, *48*, 463-487.

[7] Peng, H.; Guo, J. *Environ. Chem. Lett.*, **2020**, *18*, 2055-2068.

[8] Bashir, A.; Malik, L. A.; Ahad, S.; Manzoor, T.; Bhat, M. A.; Dar, G.; Pandith, A. H. *Environ. Chem. Lett.*, **2019**, *17*, 729-754.

[9] Beaugeard, V.; Muller, J.; Graillot, A.; Ding, X.; Robin, J.-J.; Monge, S. *React. Funct. Polym.*, **2020**, *152*, 104599.

[10] Burakov, A. E.; Galunin, E. V.; Burakova, I. V.; Kucherova, A. E.; Agarwal, S.; Tkachev, A. G.; Gupta, V. K. *Ecotoxicol. Environ. Saf.*, **2018**, *148*, 702-712.

[11] Ogunsona, E.; Ojogbo, E.; Mekonnen, T. *Polym. J.*, **2018**, *108*, 570-581.

[12] Singh, N.; Nagpal, G.; Agrawal, S. *Environ. Technol. Innovation*, **2018**, *11*, 187-240.

[13] Abdelhamid, H. N.; Mathew, A. P. *Coord. Chem. Rev.*, **2022**, *451*, 214263.

[14] Ibrahim, Y.; Abdulkarem, E.; Naddeo, V.; Banat, F.; Hasan, S. W. *Sci. Total Environ.*, **2019**, *690*, 167-180.

[15] Garba, M. D.; Usman, M.; Mazumder, M. A. J.; Al-Ahmed, A. *Environ. Chem. Lett.*, **2019**, *17*, 1195-1208.

[16] Bhadra, J.; Alkareem, A.; Al-Thani, N. *J. Polym. Res.*, **2020**, *27*, 1-20.

[17] Kekes, T.; Kolliopoulos, G.; Tzia, C. *J. Environ. Chem. Eng.*, **2021**, *9*, 105581.

[18] Manafi, M. R.; Manafi, P.; Pircheraghi, G. *Iran. J. Polym. Sci. Technol.*, **2017**, *30*, 207-219.

[19] Manafi, M.; Manafi, P.; Agarwal, S.; Bharti, A. K.; Asif, M.; Gupta, V. K. *J. Colloid Interface Sci.*, **2017**, *490*, 505-510.

[20] Olad, A.; Doustdar, F.; Gharekhani, H. *Colloids Surf., A*, **2020**, *601*, 124962.

[21] Alam, A.; Zhang, Y.; Kuan, H.-C.; Lee, S.-H.; Ma, J. *Prog. Polym. Sci.*, **2018**, *77*, 1-18.

[22] Buruga, K.; Song, H.; Shang, J.; Bolan, N.; Jagannathan, T. K.; Kim, K.-H. *J. Hazard. Mater.*, **2019**, *379*, 120584.

[23] Rivas, B. L.; Pereira, E.; Maureira, A. *Polym. Int.*, **2009**, *58*, 1093-1114.

[24] Mignon, A.; De Belie, N.; Dubruel, P.; Van Vlierberghe, S. *Eur. Polym. J.*, **2019**, *117*, 165-178.

[25] Song, X.; An, J.; He, C.; Zhou, J.; Xu, Y.; Ji, H.; Yang, L.; Yin, J.; Zhao, W.; Zhao, C. *J. Mater. Chem. A*, **2019**, *7*, 21386-21403.

[26] Bhagat, S. K.; Paramasivan, M.; Al-Mukhtar, M.; Tiyasha, T.; Pyrgaki, K.; Tung, T. M.; Yaseen, Z. M. *Environ. Sci. Pollut. Res.*, **2021**, *28*, 31670-31688.

[27] Godiya, C. B.; Ruotolo, L. A. M.; Cai, W. *J. Mater. Chem. A*, **2020**, *8*, 21585-21612.

[28] Mincke, S.; Asere, T. G.; Verheye, I.; Folens, K.; Bussche, F. V.; Lapeire, L.; Verbeken, K.; Van Der Voort, P.; Tessema, D. A.; Fufa, F. *Green Chem.*, **2019**, *21*, 2295-2306.

[29] Sinha, V.; Chakma, S. *J. Environ. Chem. Eng.*, **2019**, *7*, 103295.

[30] Van Tran, V.; Park, D.; Lee, Y.-C. *Environ. Sci. Pollut. Res.*, **2018**, *25*, 24569-24599.

[31] Qamruzzaman, M.; Ahmed, F.; Mondal, M.; Ibrahim, H. *J. Polym. Environ.,* **2022**, *30*, 19-50.

[32] Reddy, D. H. K.; Lee, S.-M. *Adv. Colloid Interface Sci.*, **2013**, *201*, 68-93.

[33] Pang, L.; Gao, Z.; Feng, H.; Wang, S.; Wang, Q. *J. Controlled Release*, **2019**, *316*, 105-115.

[34] Wang, J.; Zhuang, S. *Crit. Rev. Environ. Sci. Technol.*, **2017**, *47*, 2331-2386.

[35] Sharma, G.; Thakur, B.; Naushad, M.; Kumar, A.; Stadler, F. J.; Alfadul, S. M.; Mola, G. T. *Environ. Chem. Lett.*, **2018**, *16*, 113-146.

[36] Pourjavadi, A.; Salimi, H.; Amini-Fazl, M.; Kurdtabar, M.; Amini-Fazl, A. *J. Appl. Polym. Sci.*, **2006**, *102*, 4878-4885.

[37] Dong, C.; Lu, J.; Qiu, B.; Shen, B.; Xing, M.; Zhang, J. *Appl. Catal.,* **2018**, *222*, 146-156.

[38] Sennakesavan, G.; Mostakhdemin, M.; Dkhar, L.; Seyfoddin, A.; Fatihhi, S. *Degrad. Stab.*, **2020**, *180*, 109308.

[39] Tran, H. N.; You, S.-J.; Chao, H.-P. *J. Environ. Chem. Eng.*, **2016**, *4*, 2671-2682.

[40] Wang, Y.; Xiong, Y.; Wang, J.; Zhang, X. *Colloids Surf., A*, **2017**, *520*, 903-913.

[41] Guo, Y.; Lu, H.; Zhao, F.; Zhou, X.; Shi, W.; Yu, G. *Adv. Mater.*, **2020**, *32*, 1907061.

[42] Badsha, M. A.; Khan, M.; Wu, B.; Kumar, A.; Lo, I. M. *J. Hazard. Mater.*, **2021**, *408*, 124463.